This is the accepted manuscript made available via CHORUS. The article has been published as:

Angular dependence of spin-orbit spin-transfer torques

Ki-Seung Lee, Dongwook Go, Aurélien Manchon, Paul M. Haney, M. D. Stiles, Hyun-Woo Lee, and Kyung-Jin Lee

Phys. Rev. B **91**, 144401 — Published 6 April 2015

DOI: 10.1103/PhysRevB.91.144401

Angular dependence of spin-orbit spin transfer torques

Ki-Seung Lee[1,**], Dongwook Go[2,**], Aurélien Manchon[3], Paul M. Haney[4], M. D. Stiles[4], Hyun-Woo Lee[2,*] and Kyung-Jin Lee[1,5†]

[1]*Department of Materials Science and Engineering, Korea University, Seoul 136-701, Korea*

[2]*PCTP and Department of Physics, Pohang University of Science and Technology, Pohang 790-784, Korea*

[3]*Physical Science and Engineering Division, King Abdullah University of Science and Technology (KAUST), Thuwal 23955-6900, Saudi Arabia*

[4]*Center for Nanoscale Science and Technology, National Institute of Standards and Technology, Gaithersburg, Maryland 20899, USA*

[5]*KU-KIST Graduate School of Converging Science and Technology, Korea University, Seoul 136-713, Korea*

In ferromagnet/heavy metal bilayers, an in-plane current gives rise to spin-orbit spin transfer torque which is usually decomposed into field-like and damping-like torques. For two-dimensional free-electron and tight-binding models with Rashba spin-orbit coupling, the field-like torque acquires nontrivial dependence on the magnetization direction when the Rashba spin-orbit coupling becomes comparable to the exchange interaction. This nontrivial angular dependence of the field-like torque is related to the Fermi surface distortion, determined by the ratio of the Rashba spin-orbit coupling to the exchange interaction. On the other hand, the damping-like torque acquires nontrivial angular dependence when the Rashba spin-orbit coupling is comparable to or stronger than the exchange interaction. It is related to the combined effects of the Fermi surface distortion and the Fermi sea contribution. The angular dependence is consistent with experimental observations and can be important to understand magnetization dynamics induced by spin-orbit spin transfer torques.

I. INTRODUCTION

In-plane current-induced spin-orbit spin transfer torques in ferromagnet/heavy metal bilayers provide an efficient way of inducing magnetization dynamics and may play a role in future magnetoelectronic devices.[1–15] Two mechanisms for spin-orbit torques have been proposed to date; the bulk spin Hall effect in the heavy metal layer[16–20] and interfacial spin-orbit coupling effect at the ferromagnet/heavy metal interface[21–31] frequently referred to as the Rashba effect. Substantial efforts have been expended in identifying the dominant mechanism for the spin-orbit torque.[30–35] For this purpose, one needs to go beyond qualitative analysis since both the mechanisms result in qualitatively identical predictions, i.e. two vector components of spin-orbit torque (see Eq. (1)). For quantitative analysis, we adopt the commonly used decomposition of the spin-orbit torque $\mathbf{T}$,

$$\mathbf{T} = \tau_{\rm f}\hat{\mathbf{M}} \times \hat{\mathbf{y}} + \tau_{\rm d}\hat{\mathbf{M}} \times (\hat{\mathbf{M}} \times \hat{\mathbf{y}}), \qquad (1)$$

where the first term is commonly called the field-like spin-orbit torque, the second term the damping-like spin-orbit torque or the Slonczewski-like spin-orbit torque, $\hat{\mathbf{M}} = (\cos\phi\sin\theta, \sin\phi\sin\theta, \cos\theta)$ is the unit vector along the magnetization direction, $\hat{\mathbf{y}}$ is the unit vector perpendicular to both current direction ($\hat{\mathbf{x}}$) and the direction in which the inversion symmetry is broken ($\hat{\mathbf{z}}$), $\tau_{\rm f}$ and $\tau_{\rm d}$ describe the magnitude of field-like and damping-like spin-orbit torque terms, respectively. Since $\mathbf{T}$ should be orthogonal to $\hat{\mathbf{M}}$, the two terms in Eq. (1), which are orthogonal to $\hat{\mathbf{M}}$ and also to each other, provide a perfectly general description of the spin-orbit torque regardless of the detailed mechanism of $\mathbf{T}$. The quantitative analysis of $\mathbf{T}$ then amounts to the examination of the properties of $\tau_{\rm f}$ and $\tau_{\rm d}$.

One of intriguing features of spin-orbit torque observed in some experiments is the strong dependence of $\tau_{\rm f}$ and $\tau_{\rm d}$ on the magnetization direction.[36,37] Comparing the measured and calculated angular dependence will provide clues to the mechanism of the spin-orbit torque. The detailed angular dependence also determines the magnetization dynamics and hence is important for device applications based on magnetization switching[1,3,10–13], domain wall dynamics[2,5–9,14,15], and magnetic skyrmion motion[38].

Theories based on the bulk spin Hall effect combined with a drift-diffusion model or Boltzmann transport equation[30] predict no angular dependence of $\tau_{\rm f}$ and $\tau_{\rm d}$, which is not consistent with the experimental results.[36,37] For theories based on the interfacial spin-orbit coupling, the angular dependence is subtle. Based on the Rashba model including D'yakonov-Perel spin relaxation, Pauyac *et al.*[39] studied the angular dependence of spin-orbit torque perturbatively in weak Rashba regime ($r \equiv \alpha_{\rm R}k_{\rm F}/J \ll 1$) and strong Rashba regime ($r \gg 1$) where $\alpha_{\rm R}$ is the strength of the Rashba spin-orbit coupling, $k_{\rm F}$ is the Fermi wave vector, and J is the exchange coupling. They found that both $\tau_{\rm f}$ and $\tau_{\rm d}$ are almost independent of the angular direction of $\hat{\mathbf{M}}$ in the weak Rashba regime. In the strong Rashba regime, on the other hand, they found that $\tau_{\rm d}$ exhibits strong angular dependence. The origin of the angular dependence within this model is the anisotropy of the spin relaxation, which arises naturally since the Rashba spin-orbit interaction is responsible for the anisotropic D'yakonov-Perel spin relaxation mechanism. For $\tau_{\rm f}$, in contrast, they found it to be almost constant in the strong Rashba regime even when the spin relaxation is anisotropic. Experimentally,[36,37] both the damping-like and the field-like contri-

butions depend strongly on the magnetization direction.

Here we reexamine the angular dependence of the spin-orbit torque based on the Rashba interaction motivated by the following two observations. The first motivation comes from a first-principles calculation[40] of Co/Pt bilayers, according to which both the spin-orbit potential and the exchange splitting are large near the interface between the heavy metal and the ferromagnet. This implies that the problem of interest is not in the analytically tractable weak Rashba or strong Rashba regime but in the intermediate Rashba regime ($r \approx 1$). We examine this intermediate regime numerically and find that in contrast to both the strong and weak Rashba regimes, $\tau_{\rm f}$ has a strong angular dependence. The second motivation comes from a recent calculation[29,31] showing that the interfacial spin-orbit coupling can generate $\tau_{\rm d}$ through a Berry phase contribution[41]. In contrast, earlier theories[26–28] of the interfacial spin-orbit coupling found a separate contribution to $\tau_{\rm d}$ from spin relaxation. Moreover those calculations[31] suggest that the Berry phase contribution to $\tau_{\rm d}$ is much larger than the spin relaxation contribution. Here, we examine the angular dependence of the Berry phase contribution.

To be specific, we examine the angular dependence of the spin-orbit torques for two-dimensional free-electron models of ferromagnetic systems with Rashba spin-orbit coupling. The model [see Eq. (2)] has two energy bands and assumes all material parameters are isotropic. While the model is drastically simplified compared to realistic materials, it reveals clearly how the competition between spin-orbit coupling and exchange coupling generates angular dependence. We expect this mechanism for the angular dependence to persist in real materials. Another reason to consider such simple models comes from the observation that the existing measurements[36,37] of the angular dependence are for granular materials. In such systems, mechanisms for anisotropy that arise explicitly from the crystallinity (or magnetocrystallinity) are likely to average to zero, leaving mechanisms related to those found in models [Eq. (2)] with isotropic material parameters.

When an electric field is applied to generate an in-plane current, the spin-orbit torque arises from the two types of changes caused by the electric field. One is the electron occupation change. For a small electric field, the net occupation change is limited to the Fermi surface so that the spin-orbit torque caused by the occupation change comes from the Fermi surface. For this reason, this contribution is referred to as the Fermi surface contribution. The other is the state change. The electric field modifies the potential energy of the system, which in turn modifies wavefunctions of all single particle states. Thus the spin-orbit torque caused by the state change comes not only from the states near the Fermi surface but also from all states in the entire Fermi sea. This contribution is referred to as the Fermi sea contribution and often closely related to the momentum-space Berry phase[31].

For the Rashba model [Eq. (2)], we find that in the absence of spin relaxation, the Fermi surface contribution to $\tau_{\rm d}$ is vanishingly small, while $\tau_{\rm f}$ remains finite. In the intermediate Rashba regime, $\tau_{\rm f}$ has a substantial angular dependence. This nontrivial angular dependence of $\tau_{\rm f}$ is related to Fermi surface distortion, which becomes significant when the Rashba spin-orbit coupling energy ($\sim \alpha_R k_F$) is comparable to the exchange coupling ($\sim J$). On the other hand, the Fermi sea contribution generates primarily $\tau_{\rm d}$ which exhibits strong angular dependence in both the intermediate and strong Rashba regimes. The nontrivial angular dependence of $\tau_{\rm d}$ is caused by the combined effects of Fermi surface distortion and the Fermi sea contribution. We also compute the angular dependence of the spin-orbit torques for a tight-binding model and find that the results are qualitatively consistent with those for a free-electron model. Lastly, we comment briefly on possible angular dependence of crystalline or magnetocrystalline origin, which we do not examine in the present study.

II. SEMICLASSICAL MODELS

In this section, we use subscripts (1) and (2) to denote the Fermi surface and the Fermi sea contributions, respectively. The model Hamiltonian for an electron in the absence of an external electric field is

$$H_0 = \frac{\mathbf{p}^2}{2m} + \alpha_{\rm R}\boldsymbol{\sigma}\cdot(\mathbf{k}\times\hat{\mathbf{z}}) + J\boldsymbol{\sigma}\cdot\hat{\mathbf{M}}, \tag{2}$$

where $\mathbf{k} = (k_x, k_y)$ is the two-dimensional wave vector, m is the electron mass, J (>0) is the exchange parameter, $\mathbf{p}$ is the momentum, and $\boldsymbol{\sigma}$ is the vector of Pauli matrices, and M_x, M_y, and M_z are the x-, y-, and z-components of $\hat{\mathbf{M}}$, respectively. When $\hat{\mathbf{M}}$ is position-independent, which will be assumed all throughout this paper, $\mathbf{k}$ is a good quantum number. For each $\mathbf{k}$, there are two energy eigenvalues since the spin may point in two different directions. Thus the energy eigenvalues of H_0 form two energy bands, called majority and minority bands. The one-electron eigenenergy of H_0 is

$$E^{\pm}_{\mathbf{k}} = \frac{\hbar^2 k^2}{2m} \mp \epsilon_{\mathbf{k}}, \tag{3}$$

where the upper (lower) sign corresponds to the majority (minority) band, $k^2 = k_x^2 + k_y^2$, and $\epsilon_{\mathbf{k}} = |J\hat{\mathbf{M}} + \alpha_{\rm R}(\mathbf{k}\times\hat{\mathbf{z}})|$.

To determine the spin state of the majority and minority bands, it is useful to combine the last two terms of H_0 into an effective Zeeman energy term ($= -\mu_B \mathbf{B}_{{\rm eff},\mathbf{k}}\cdot\boldsymbol{\sigma}$), where the effective magnetic field is $\mathbf{k}$-dependent and given by

$$\mathbf{B}_{{\rm eff},\mathbf{k}} = -\frac{J}{\mu_{\rm B}}\hat{\mathbf{M}} - \frac{\alpha_{\rm R}}{\mu_{\rm B}}(\mathbf{k}\times\hat{\mathbf{z}}). \tag{4}$$

Here $\mu_{\rm B}$ is the Bohr magneton. $\mathbf{B}_{{\rm eff},\mathbf{k}}$ fixes the spin direction of the majority and minority bands. For the

eigenstate $|\psi_{\mathbf{k},\pm}\rangle$ in the majority/minority band, its spin expectation value $\mathbf{s}^{\pm}_{\mathbf{k}(1)} \equiv (\hbar/2)\langle\psi_{\mathbf{k},\pm}|\boldsymbol{\sigma}|\psi_{\mathbf{k},\pm}\rangle$ is given by

$$\mathbf{s}^{\pm}_{\mathbf{k}(1)} = \pm\frac{\hbar}{2}\hat{\mathbf{B}}_{\mathrm{eff},\mathbf{k}}, \tag{5}$$

where $\hat{\mathbf{B}}_{\mathrm{eff},\mathbf{k}}$ is the unit vector along $\mathbf{B}_{\mathrm{eff},\mathbf{k}}$. In terms of the $\mathbf{k}$-dependent angle $\theta_{\mathbf{k}}$ and $\phi_{\mathbf{k}}$, which are defined by $\hat{\mathbf{B}}_{\mathrm{eff},\mathbf{k}} = (\sin\theta_{\mathbf{k}}\cos\phi_{\mathbf{k}}, \sin\theta_{\mathbf{k}}\sin\phi_{\mathbf{k}}, \cos\theta_{\mathbf{k}})$, the eigenstate $|\psi_{\mathbf{k},\pm}\rangle$ is given by

$$|\psi_{\mathbf{k},+}\rangle = \mathrm{e}^{i\mathbf{k}\cdot\mathbf{r}}\begin{pmatrix}\cos(\theta_{\mathbf{k}}/2)\\ \sin(\theta_{\mathbf{k}}/2)\mathrm{e}^{i\phi_{\mathbf{k}}}\end{pmatrix} \tag{6}$$

$$|\psi_{\mathbf{k},-}\rangle = \mathrm{e}^{i\mathbf{k}\cdot\mathbf{r}}\begin{pmatrix}\sin(\theta_{\mathbf{k}}/2)\\ -\cos(\theta_{\mathbf{k}}/2)\mathrm{e}^{i\phi_{\mathbf{k}}}\end{pmatrix} \tag{7}$$

Together with the energy eigenvalue $E^{\pm}_{\mathbf{k}}$ in Eq. (3), the eigenstate $|\psi_{\mathbf{k},\pm}\rangle$ completely specifies properties of the equilibrium Hamiltonian. The ground state of the system is then achieved by filling up all single particle eigenstates $|\psi_{\mathbf{k},\pm}\rangle$, below the Fermi energy E_F.

When an electric field $\mathbf{E} = E\hat{\mathbf{x}}$ is applied, one of the effects is the modification of the state occupation. This effect generates the non-equilibrium spin density $\mathbf{s}^{\pm}_{(1)}$ as

$$\mathbf{s}^{\pm}_{(1)} = \int\frac{dk^2}{(2\pi)^2}\left[f_{\pm}\left(\mathbf{k} - \frac{eE\tau}{\hbar}\hat{\mathbf{x}}\right) - f_{\pm}(\mathbf{k})\right]\mathbf{s}^{\pm}_{\mathbf{k}(1)}, \tag{8}$$

where $-e$ is the electron charge, τ is the relaxation time, and $f_{\pm}(\mathbf{k}) = \Theta(E_F - E^{\pm}_{\mathbf{k}})$ is the zero-temperature electron occupation function where $\Theta(x)$ is the Heaviside step function. Note that the net contribution to $\mathbf{s}^{\pm}_{(1)}$ arises entirely from the states near E_F due to the cancellation effect between the two occupation functions in Eq. (8). Thus $\mathbf{s}^{\pm}_{(1)}$ is a *Fermi surface* contribution. The total spin density generated by the occupation change becomes $\mathbf{s}_{(1)} = \mathbf{s}^{+}_{(1)} + \mathbf{s}^{-}_{(1)}$. This is related to the spin-orbit torque $\mathbf{T}_{(1)}$ generated by the occupation change via $\mathbf{T}_{(1)} = (J/\hbar)\mathbf{s}_{(1)}\times\hat{\mathbf{M}}$. In Eq. (8), we use the relaxation time approximation with the assumption that the scattering probability is isotropic and spin-independent.

The other important effect of the electric field other changing than the occupation is that it modifies the potential energy that the electrons feel, and hence modifies their wave functions, generating in turn a correction to $\mathbf{s}^{\pm}_{\mathbf{k}(1)}$. We call this correction $\mathbf{s}^{\pm}_{\mathbf{k}(2)}$. It is calculated in Appendix A and given by

$$\mathbf{s}^{\pm}_{\mathbf{k}(2)} = \pm\frac{\hbar}{2}\alpha_R eE\left[\frac{J}{2\epsilon^3_{\mathbf{k}}}(\hat{\mathbf{M}}\times\hat{\mathbf{y}}) + \frac{\alpha_R}{2\epsilon^3_{\mathbf{k}}}(\hat{\mathbf{x}}\times\mathbf{k})\right]. \tag{9}$$

Summing over all occupied states in the majority/minority band, gives the total spin density $\mathbf{s}^{\pm}_{(2)}$ generated by the state change in that band, and is given by

$$\mathbf{s}^{\pm}_{(2)} = \int\frac{dk^2}{(2\pi)^2}f_{\pm}(\mathbf{k})\mathbf{s}^{\pm}_{\mathbf{k}(2)}. \tag{10}$$

Note that the equilibrium occupation function f appears in Eq. (10) rather than the difference between the two occupation functions. The occupation change effect is ignored in Eq. (10) since we are interested in linear effects of the electric field E and $\mathbf{s}^{\pm}_{\mathbf{k}(2)}$ is already first order in E. Note that all the occupied single particle states in the Fermi sea contribute to $\mathbf{s}^{\pm}_{(2)}$. Thus $\mathbf{s}^{\pm}_{(2)}$ amounts is a *Fermi sea* contribution. The total spin density generated by the state change becomes $\mathbf{s}_{(2)} = \mathbf{s}^{+}_{(2)} + \mathbf{s}^{-}_{(2)}$. This is related to the spin-orbit torque $\mathbf{T}_{(2)}$ generated by the state change via $\mathbf{T}_{(2)} = (J/\hbar)\mathbf{s}_{(2)}\times\hat{\mathbf{M}}$.

A few remarks are in order. In Eq. (8), the two occupation functions cancel each other for most $\mathbf{k}$ values. They do not cancel for $\mathbf{k}$ points that correspond to electron excitation slightly above the Fermi surface or the hole excitation slightly below the Fermi surface. Thus the direction of $\mathbf{s}^{\pm}_{(1)}$ can be estimated simply by evaluating the difference of $\mathbf{B}_{\mathrm{eff},\mathbf{k}}$ between two $\mathbf{k}$'s of electron-like and hole-like excitations. This shows that $\mathbf{s}^{\pm}_{(1)}$ points along $E\hat{\mathbf{x}}\times\hat{\mathbf{z}} = -E\hat{\mathbf{y}}$. Thus the spin-orbit torque $\mathbf{T}_{(1)}$ should be proportional to $E\hat{\mathbf{y}}\times\hat{\mathbf{M}}$, which is nothing but the field-like spin-orbit torque. Thus the Fermi surface contribution $\mathbf{T}_{(1)}$ contributes mostly to τ_{f}. To be precise, however, this statement is not valid for spin-dependent scattering, which we neglect in deriving Eq. (8). If the scattering is spin-dependent, $\mathbf{T}_{(1)}$ produces τ_{d} as well as τ_{f} as demonstrated in Refs. 26–28. In this paper, we neglect the contribution to the angular dependence of τ_{d} from $\mathbf{T}_{(1)}$ and spin-dependent scattering since it has been already treated in Ref. 39. The contribution to τ_{d} in our study comes from the Fermi sea contribution $\mathbf{T}_{(2)}$. One can easily verify that the first term in Eq. (9) generates the spin-orbit torque proportional to $(\hat{\mathbf{M}}\times\hat{\mathbf{y}})\times\hat{\mathbf{M}}$, which has the form of the damping-like spin-orbit torque. The second term in Eq. (9) on the other hand almost vanishes upon $\mathbf{k}$ integration in Eq. (10). This demonstrates that the Fermi sea contribution $\mathbf{T}_{(2)}$ contributes mostly to τ_{d}.

We also compute the spin-orbit torques based on a tight-binding model because free electron models with linear Rashba coupling, like that we use here, can exhibit pathological behavior when accounting for vertex corrections to the impurity scattering. For example, the intrinsic spin Hall effect[41], that has the same physical origin of the Fermi sea contribution to spin-orbit torque, gives a universal result that vanishes when vertex corrections are included.[42–46] However, the intrinsic spin Hall effect does not vanish when the electron dispersion deviates from free electron behavior or the spin-orbit coupling is not linear in momentum.[47–50] Since we neglect vertex corrections in the calculations presented in this paper, it is necessary to check whether or not the angular dependence of spin-orbit torque obtained in a free-electron model is

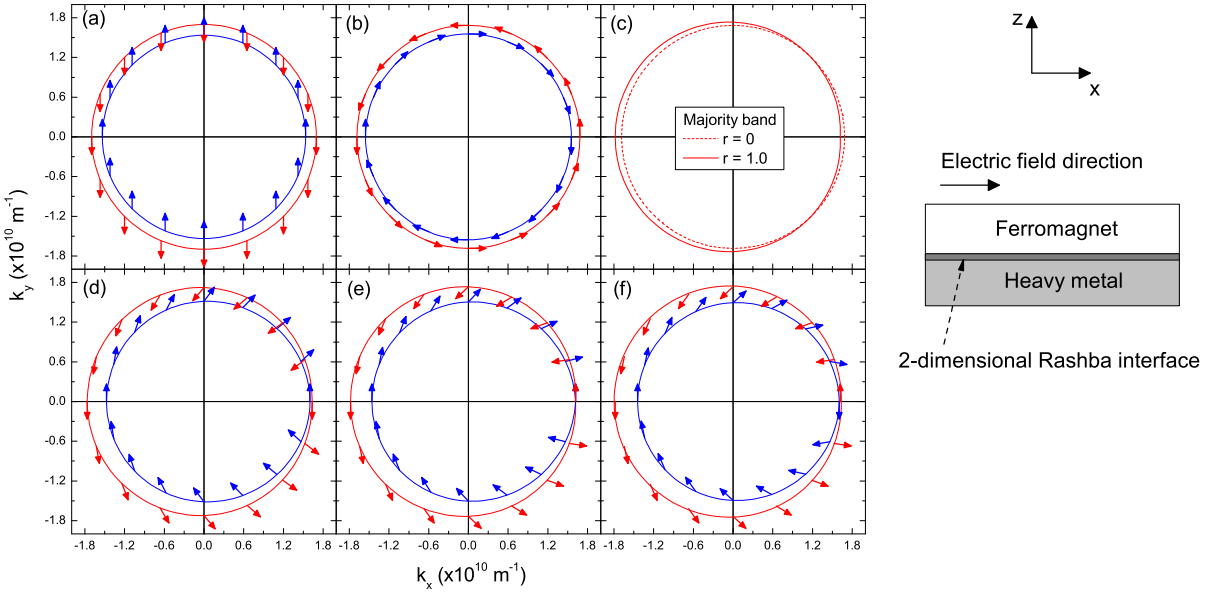

FIG. 1: (color online) Fermi surface and spin direction for a free-electron model. (a) $r = 0$ (only exchange splitting), (b) $r = \infty$ (only Rashba spin-orbit coupling and non-magnetic), (c) comparison of Fermi surfaces (majority band) for $r = 0$ and $r = 1.0$, (d) $r = 0.8$, (e) $r = 1.0$, and (f) $r = 1.2$. We assume $\hat{\mathbf{M}} = (0, 1, 0)$, $E_{\rm F}$= 10 eV, $m = m_0$, and J= 1 eV. Here m_0 is the free electron mass. The outer red (inner blue) Fermi surface corresponds to majority (minority) band. Arrows are the eigendirections of spins on the Fermi surface. The coordinate system is shown on the right.

qualitatively reproduced in a tight-binding model, where the electron dispersion deviates from free electron behavior and the spin-orbit coupling is not strictly linear in momentum. To compute spin-orbit torque in the two-band (majority and minority spin bands) tight-binding model on a square lattice with the lattice constant a, we replace k_x and k_y by $\sin(k_x a)/a$ and $\sin(k_y a)/a$, respectively. The corresponding spin density is then calculated by integrating the electric field-induced spin expectation value up to the point of band filling. For most cases in a tight-binding model, the result converges for a $\mathbf{k}$-point mesh with mesh spacing dk=0.026 nm^{-1} and 320,000 $\mathbf{k}$-points, where the convergence criteria is 1 percent change of results with a finer mesh by factor of 2. All results presented in this paper are converged to this criteria.

III. RESULTS AND DISCUSSION

We first discuss Fermi surface distortion as a function of $r(= \alpha_{\rm R} k_{\rm F}/J)$. When the Fermi surfaces are not circular, we define $k_{\rm F}$ through its relation with the electron density n; $k_{\rm F}^2 = 2\pi n$. Figure 1 shows the Fermi surface and the spin direction at each $\mathbf{k}$-point for various values of the ratio r. Without Rashba spin-orbit coupling ($r = 0$), the spin direction does not depend on $\mathbf{k}$ for ferromagnetic systems (Fig. 1(a)). Without exchange coupling (non-magnetic Rashba system ($r = \infty$)), on the other hand, the spins point in the azimuthal direction (Fig. 1(b)). For these extreme cases, the Fermi surfaces of two bands are concentric circles.

The Fermi surfaces distort significantly when $r \approx 1$. Figure 1(c) compares two Fermi surfaces (majority band) for $r = 0$ and $r = 1.0$ when $\hat{\mathbf{M}} = (0, 1, 0)$. When the magnetization has an in-plane component as in this case, each sheet of the Fermi surface shifts in a different direction and distorts from perfect circularity (Fig. 1(c): note that the dotted Fermi surface is for $r = 0$ and is a circle). This distortion arises because the $\mathbf{k}$-dependent effective magnetic field (Eq. (4)) contains contributions both from the exchange and Rashba spin-orbit couplings. An effective field from the exchange is aligned along $\hat{\mathbf{M}}$ and uniform regardless of $\mathbf{k}$, whereas that from the Rashba spin-orbit coupling lies in the $x - y$ plane and is $\mathbf{k}$-dependent. For example, for $\hat{\mathbf{M}} = (0, 1, 0)$ and majority band, an effective field from the Rashba spin-orbit coupling is parallel (anti-parallel) to that from the exchange at $\mathbf{k} = (k_{F,1}, 0)$ ($\mathbf{k} = (k_{F,2}, 0)$), where $k_{F,1}$ (> 0) and $k_{F,2}$ (< 0) are the Fermi wave vectors corresponding to the electric field-induced electron-like and hole-like excitations, respectively. The $\mathbf{k}$-dependent effective field distorts the Fermi surface distortion as demonstrated in Fig. 1(c)-(f).

This Fermi surface distortion also affects the spin direction at each $\mathbf{k}$-point because the spin eigendirection is $\mathbf{k}$-dependent due to the Rashba spin-orbit coupling. In the weak (strong) Rashba regime, the spin landscape is similar with that in Fig. 1(a) (Fig. 1(b)). In these extreme cases, the spin landscape is not significantly modified by the change in the magnetization direction as one of the effective fields (either from the exchange or from

the Rashba spin-orbit coupling) is much stronger than the other. As a result, $\tau_{\rm f}$ has almost no angular distortion in these regimes. The spin landscape for $r \approx 1$ on the other hand becomes highly complicated (Fig. 1(d)-(f)) as the Fermi surface distortion is maximized. One can easily verify that the spin landscape for $r \approx 1$ varies significantly with the magnetization direction because the Fermi surface distortion is closely related to the in-plane component of the magnetization as explained above.

As the non-equilibrium spin density corresponding to $\tau_{\rm f}$ (i.e. $\mathbf{s}_{(1)}$) is obtained from the integration of the spins on the Fermi surface, this magnetization-angle-dependent change in the spin landscape generates a nontrivial angular dependence of $\tau_{\rm f}$. A similar argument is valid for $\tau_{\rm d}$ (i.e. $\mathbf{s}_{(2)}$) which comes from the Fermi sea contribution because the Fermi surface distortion affects the interval of the integration. Therefore, the results shown in Fig. 1 suggest that the spin-orbit torque originating from the interfacial spin-orbit coupling should have a strong dependence on the magnetization angles θ and ϕ when r is close to 1.

Several additional remarks for the Fermi surface distortion are as follows. First, the two Fermi surfaces touch exactly for $r = 1$ (Fig. 1(e)) and they anticross for $r > 1$ (Fig. 1(f)). As a result, the spin landscape rapidly changes when r varies around 1 so that a similar drastic change in the angular dependence of the spin-orbit torque is expected. Second, all effects from the Fermi surface distortion, described for a free-electron model above, should also affect the results obtained for a tight-binding model. However, as the shape of the Fermi surface is different for the two models (i.e. for $J = 0$ and $\alpha_R = 0$, the Fermi surface for a free-electron model is a circle, whereas that for a tight-binding model with half band-filling is a rhombus), the results for the two models are quantitatively different.

We next show the angular dependence of $\tau_{\rm f}$ and $\tau_{\rm d}$ for the two models. Here we do not attempt to analyze the detailed angular dependence quantitatively, because it is very parameter sensitive. In contrast, our intention is to identify the general trends that emerge from these numerical calculations. Figure 2 shows the angular dependence of $\tau_{\rm f}$ for a free-electron model ((a) and (b)) and a tight-binding model ((c) and (d)). In both models, we obtain nontrivial angular dependence of $\tau_{\rm f}$ in certain parameter regimes. In the free-electron model, we find $\tau_{\rm f}$ is almost constant in the weak ($r \ll 1$) and strong ($r \gg 1$) Rashba regimes, consistent with earlier works.[23,24] In the intermediate Rashba regimes, however, $\tau_{\rm f}$ is not a constant. We find that $\tau_{\rm f}$ depends not only on the polar angle θ but also the azimuthal angle ϕ, as expected from the Fermi surface distortion (Fig. 1). In Fig. 2(b), $\tau_{\rm f}$ for $r < 1$ ($r > 1$) is maximal (minimal) at $\theta = \pi/2$, which is caused by the anticrossing of the two Fermi surfaces (Fig. 1(d)-(f)). Despite the strong angular dependence, the sign of $\tau_{\rm f}$ is preserved since the spin direction of nonequilibrium spin density is unambiguously determined once the direction of electric field and the sign of $\alpha_{\rm R}$ are fixed.

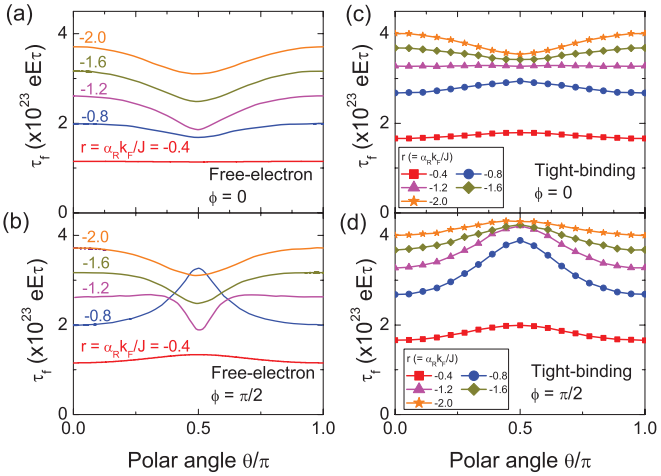

FIG. 2: (color online) Polar angle (θ) dependence of field-like spin-orbit torque coefficient $\tau_{\rm f}$. Free-electron model (a and b): (a) azimuthal angle of magnetization $\phi = 0$ and (b) $\phi = \pi/2$. Tight-binding model (c and d): (c) $\phi = 0$ and (d) $\phi = \pi/2$. For both models, we use E_F= 4 eV, $m = m_0$, and J= 1 eV. For a tight-binding model, we use $a = 0.25$ nm.

These overall trends are qualitatively reproduced in a tight-binding model (Fig. 2(c) and (d)). The magnitude and angular dependence of $\tau_{\rm f}$ differ quantitatively from those of the free electron model, due to the different shape of the Fermi surfaces for the two models. In contrast to the almost circular Fermi surfaces (centered almost at $\mathbf{k} = 0$) of the free-electron model (Fig. 1), the Fermi surfaces of the tight-binding model have different shapes depending on the electron density; when a given band is only weakly filled, half filled, or almost fully filled, the corresponding Fermi surface has a circular shape centered at the Γ point ($\mathbf{k} = 0$), a diamond shape, or a circular shape centered at the M point [$\mathbf{k} = (\pi/2a, \pi/2a)$], respectively. Such Fermi surface shape variation is accompanied by spin configuration differences between the two models. For instance, whereas the Rashba spin-orbit coupling $\alpha_{\rm R}\boldsymbol{\sigma} \cdot (\mathbf{k} \times \hat{\mathbf{z}}) = \alpha_{\rm R}(\sigma_x k_y - \sigma_y k_x)$ for the free-electron model vanishes only at the Γ point, the Rashba spin-orbit coupling $(\alpha_{\rm R}/a)[\sigma_x \sin(k_y a) - \sigma_y \sin(k_x a)]$ for the tight-binding model vanishes not only at the Γ point but also at the M point and the X points [$\mathbf{k} = (0, \pi/2a)$ and $(\pi/2a, 0)$].

Figure 3 shows the angular dependence of $\tau_{\rm d}$ for a free-electron model ((a) and (b)) and a tight-binding model ((c) and (d)). This $\tau_{\rm d}$ results from the Fermi sea contribution (Eqs. (9) and (10)). In both models, we obtain nontrivial angular dependence of $\tau_{\rm d}$ both in the intermediate and strong Rashba regimes (Fig. 3(a) and (c)). This is in contrast to $\tau_{\rm f}$ which exhibits nontrivial angular dependence only in the intermediate Rashba regime. To understand this difference, we derive an approximate $\tau_{\rm d}$ by expanding up to third order in $\frac{\alpha_R k_F}{J}$ and assuming no Fermi surface distortion (i.e. the Fermi wave vector k_F does not depend on the direction of $\mathbf{k}$), which is analyt-

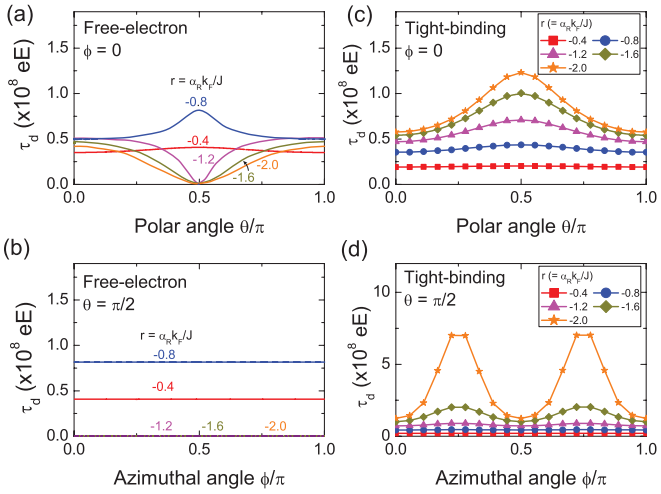

FIG. 3: (color online) Angular dependence of damping-like spin-orbit torque coefficient $\tau_{\rm d}$. Free-electron model (a and b): (a) polar angle dependence at $\phi = 0$ and (b) azimuthal angle dependence at $\theta = \pi/2$. Lines for $r = -1.2$, -1.6, and -2.0 are not clearly visible since $\tau_{\rm d} = 0$ for these cases. Tight-binding model (c and d): (c) polar angle dependence at $\phi = 0$ and (d) azimuthal angle dependence at $\theta = \pi/2$. Same parameters are used as in Fig. 2.

ically tractable. By integrating Eq. (10) with these assumptions, we find $\tau_{\rm d} \propto (16J^2 - 3\alpha_R^2 k_F^2 - 9\alpha_R^2 k_F^2 \cos(2\theta))$. Therefore, the Fermi sea contribution induces an intrinsic angular dependence in $\tau_{\rm d}$, which increases with $\frac{|\alpha_R| k_F}{J}$ irrespective of the Fermi surface distortion. The results in Fig. 3, which are obtained numerically, include the Fermi surface distortion, so that the nontrivial angular dependence of $\tau_{\rm d}$ results from the combined effects of the intrinsic Fermi sea contribution and the Fermi surface distortion. For example, Fig. 3(a) shows a sharp difference in the angular dependence of $\tau_{\rm d}$ for $r > 1$ and $r < 1$. This is qualitatively similar to the results of $\tau_{\rm f}$ shown in Fig. 2(b), showing that the Fermi surface distortion (together with the accompanying spin configuration change) also has a role in the angular dependence of $\tau_{\rm d}$.

The sign of $\tau_{\rm d}$ does not change with the magnetization angle despite the strong angular dependence, similar to the behavior of $\tau_{\rm f}$. When $\theta = \pi/2$ (Fig. 3(d)), a steep increase of $\tau_{\rm d}$ is obtained at $\phi = \pi/4$ and $3\pi/4$, originating from the shape of the Fermi surface. We expect that this strong dependence of $\tau_{\rm d}$ on ϕ can be observed in epitaxial bilayers but may be absent in sputtered bilayers as sputtered thin films consist of small grains with different lattice orientation in the film plane. However, the dependence of $\tau_{\rm d}$ on the polar angle θ (Fig. 3(a) and (c)) is irrelevant to this in-plane crystallographic issue so we expect that it will be observable in experiments when the interfacial spin-orbit coupling is comparable to or stronger than the exchange coupling. We note that a strong dependence of $\tau_{\rm d}$ on θ (but a very weak dependence on ϕ) was experimentally observed in sputtered bilayers.[36]

We finally illustrate the connection between $\tau_{\rm d}$ (i.e. $\mathbf{T}_{(2)}$) and the Berry phase. This examination is motivated by Ref. 31, which called $\mathbf{T}_{(2)}$ the Berry phase contribution. To clarify the connection, it is useful to express the Fermi sea contribution $\mathbf{s}_{(2)}$ in the Kubo formula form,

$$\mathbf{s}_{(2)} = \frac{1}{2} e E \hbar^2 A \mathrm{Im} \sum_{ab} \int \frac{d^2k}{(2\pi)^2} \left[f_a(\mathbf{k}) - f_b(\mathbf{k}) \right] \frac{\langle \mathbf{k}, a | \boldsymbol{\sigma} | \mathbf{k}, b \rangle \langle \mathbf{k}, b | v_x | \mathbf{k}, a \rangle}{\left[E_a(\mathbf{k}) - E_b(\mathbf{k}) + 2i\delta \right]^2}, \tag{11}$$

where a, b are band indices, and δ is an infinitesimally small positive constant. In the present case, $|\mathbf{k}, a\rangle$ is either $|\psi_{\mathbf{k},+}\rangle$ or $|\psi_{\mathbf{k},-}\rangle$. One then uses the relations

$$v_x = \frac{1}{\hbar} \frac{\partial H_0(\mathbf{k}, \mathbf{M})}{\partial k_x}, \quad \sigma_\alpha = \frac{1}{J} \frac{\partial H_0(\mathbf{k}, \mathbf{M})}{\partial M_\alpha}, \tag{12}$$

where the notation $H_0(\mathbf{k}, \mathbf{M})$ emphasizes that the unperturbed Hamiltonian H_0 is a function of the momentum $\mathbf{k}$ and the magnetization $\mathbf{M}$. Note that here we use $\mathbf{M}$ instead of $\hat{\mathbf{M}}$ since one needs to relax the constraint $|\hat{\mathbf{M}}| = 1$ to establish the connection with the Berry phase. Equation (12) allows one to convert the numerator of Eq. (11) as follows,

$$\langle \mathbf{k}, a | \boldsymbol{\sigma} | \mathbf{k}, b \rangle = -\frac{1}{J} \left[E_a(\mathbf{k}) - E_b(\mathbf{k}) \right] \langle \mathbf{k}, a | \nabla_{\mathbf{M}} | \mathbf{k}, b \rangle, \quad \langle \mathbf{k}, b | v_x | \mathbf{k}, a \rangle = -\frac{1}{\hbar} \left[E_b(\mathbf{k}) - E_a(\mathbf{k}) \right] \langle \mathbf{k}, b | \frac{\partial}{\partial k_x} | \mathbf{k}, a \rangle. \tag{13}$$

Thus the numerator of Eq. (11) acquires the factor $[E_a(\mathbf{k}) - E_b(\mathbf{k})]^2$, which cancels the denominator in the

limit $\delta \to 0$. Then one of the two summations for the band indices a and b can be performed to produce

$$[\mathbf{s}_{(2)}]_\alpha = \frac{1}{2}\frac{eE\hbar A}{J}\sum_a \int \frac{d^2k}{(2\pi)^2} f_a(\mathbf{k}) \left[\frac{\partial}{\partial k_x}\mathcal{A}^a_{M_\alpha}(\mathbf{k}) - \frac{\partial}{\partial M_\alpha}\mathcal{A}^a_{k_x}(\mathbf{k})\right], \tag{14}$$

where the spin-space Berry phase $\mathcal{A}^a_{M_\alpha}(\mathbf{k})$ and the momentum-space Berry phase $\mathcal{A}^a_{k_x}(\mathbf{k})$ are defined by

$$\begin{aligned} \mathcal{A}^a_{M_\alpha}(\mathbf{k}) &= i\langle \mathbf{k}, a|\frac{\partial}{\partial M_\alpha}|\mathbf{k}, a\rangle \\ \mathcal{A}^a_{k_x}(\mathbf{k}) &= i\langle \mathbf{k}, a|\frac{\partial}{\partial k_x}|\mathbf{k}, a\rangle. \end{aligned} \tag{15}$$

Here these Berry phases are manifestly real. Equation (14) establishes the connection between $\mathbf{T}_{(2)}$ and the spin-momentum-space Berry phase.

A few remarks are in order. First, through an explicit evaluation of the Berry phases, one can verify that the integrand of Eq. (14) generates $\mathbf{s}^{\pm}_{\mathbf{k}(2)}$ in Eq. (9) precisely. Second, Eq. (14) contains the occupation function $f_a(\mathbf{k})$ itself rather than difference between the occupation functions or derivatives of the occupation function. Thus $\mathbf{s}_{(2)}$ may be classified as a Fermi sea contribution. We note, however, that the Fermi sea contribution Eq. (14) may be converted to a different form[51], where the net contribution is evaluated only at the Fermi surface. To demonstrate this point, we integrate Eq. (14) by parts, which generates

$$[\mathbf{s}_{(2)}]_\alpha = \frac{1}{2}\frac{eE\hbar A}{J}\sum_a \int \frac{d^2k}{(2\pi)^2} \left[-\frac{\partial f_a(\mathbf{k})}{\partial k_x}\mathcal{A}^a_{M_\alpha}(\mathbf{k}) + \frac{\partial f_a(\mathbf{k})}{\partial M_\alpha}\mathcal{A}^a_{k_x}(\mathbf{k})\right]. \tag{16}$$

Note that in the zero temperature limit, both $\partial f_a(\mathbf{k})/\partial k_x$ and $\partial f_a(\mathbf{k})/\partial M_\alpha$ are nonzero only at the Fermi surface, and thus the net contribution to $\mathbf{s}_{(2)}$ depends only on properties evaluated at the Fermi surface. In this sense, this Fermi surface contribution is analogous to Friedel oscillations. Friedel oscillations form near surfaces when electrons reflect and the incoming and outgoing waves interfere. Then, each electron below the Fermi energy makes an oscillatory contribution to the density with a wavelength that depends on the energy. However, integrating up from the bottom of the band to the Fermi energy gives a result that only depends on the properties of the electrons at the Fermi energy where there is a sharp cut-off in the integration.

IV. SUMMARY

We use simple models to examine the angular dependence of spin-orbit torques as a function of the ratio of the spin-orbit interaction to the exchange interaction. We find that both the field-like and damping-like torques are angle independent when the spin-orbit coupling is weak but become angle-dependent when the spin-orbit coupling becomes comparable to the exchange coupling. When the spin-orbit coupling becomes much stronger than the exchange coupling, the angular dependence of the field-like torque goes away, but that of the damping-like torque remains. The angular dependence of the field-like torque becomes significant when the spin-orbit coupling becomes strong enough to distort the Fermi surface so that it changes when the direction of the magnetization changes. On the other hand, the angular dependence of the damping-like torque is caused by the combined effects of the intrinsic Fermi sea contribution and the Fermi surface distortion. We expect that these qualitative conclusions will hold for more realistic treatments of the interface. The strong angular dependence of the spin-orbit torques will significantly impact their role in large amplitude magnetization dynamics like switching or domain wall motion. This suggests caution when comparing measurement of the strength of torques with the magnetizations in different directions.

Lastly, we comment on possible other sources of angular dependence. In crystalline materials, the Rashba spin-orbit coupling coefficient $\alpha_{\rm R}$ may depend[52] on the angular direction of the magnetization $\hat{\mathbf{M}}$ and the exchange coupling coefficient J may not be strictly isotropic. Such angular dependence in spin-related coefficients will generate additional angular dependence to $\tau_{\rm f}$ and $\tau_{\rm d}$, which may show up even in the weak Rashba regime. We neglect such effects in the present calculation. Experimentally testing for angular dependence of crystalline (or magnetocrystalline) origin, would require

high quality crystalline samples in contrast to existing experimental measurements[36,37] of the angular dependence of $\tau_{\rm f}$ and $\tau_{\rm d}$ for granular materials, where the angular dependence of crystalline origin is expected to average out.

Acknowledgments

K.-J.L. acknowledges support from the NRF (2011-028163, NRF-2013R1A2A2A01013188) and under the Cooperative Research Agreement between the University of Maryland and the National Institute of Standards and Technology Center for Nanoscale Science and Technology, Award 70NANB10H193, through the University of Maryland. H.-W.L. was supported by NRF (2013R1A2A2A05006237) and MOTIE (Grant No. 10044723). A.M. acknowledges support by the King Abdullah University of Science and Technology. D.G. acknowledges support from the Global Ph.D. Fellowship Program funded by NRF (2014H1A2A101).

Appendix A: Derivation of Eq. (9)

Here, we derive the Fermi sea contribution of the spin-orbit torque. First, we calculate the change of the eigenstates in the presence of an external electric field. Second, we calculate the resulting spin accumulation. We use time-dependent perturbation theory, adiabatically turning on the electric field, which is treated as the perturbation. We adopt time-dependent perturbation approach instead of the Kubo formula for pedagogical reasons since it directly shows how the states change due to the perturbation. One can show that both approaches give the same result.

Let us consider an in-plane electric field $\mathbf{E}'(t) = \mathbf{E}\exp(\delta t)$, where $\exp(\delta t)$ gives the adiabatic turning-on process. The electric field starts to increase from $t=-\infty$ until $t=0$, for very small δ which will be set to be zero at the end of the calculation. This is represented by the vector potential $\mathbf{A} = -t\exp(\delta t)\mathbf{E}$ since $\mathbf{E} = -\partial\mathbf{A}/\partial t$. In the presence of a vector potential, the momentum operator $\mathbf{p}$ is replaced by $\mathbf{p}+e\mathbf{A}$. Thus, the total Hamiltonian becomes

$$\begin{aligned} H &= \frac{(\mathbf{p}+e\mathbf{A})^2}{2m} + \frac{\alpha_R}{\hbar}\boldsymbol{\sigma}\cdot[(\mathbf{p}+e\mathbf{A})\times\hat{\mathbf{z}}] + J\boldsymbol{\sigma}\cdot\hat{\mathbf{M}} \\ &= H_0 + H_1(t) + \mathcal{O}(\mathbf{E}^2) \end{aligned} \tag{A1}$$

where

$$\begin{aligned} H_1(t) = &-\frac{e(\mathbf{E}\cdot\mathbf{p})}{m}t\exp(\delta t) \\ &+ \frac{\alpha_R}{\hbar}[(e\mathbf{E}\times\boldsymbol{\sigma})\cdot\hat{\mathbf{z}}]t\exp(\delta t). \end{aligned} \tag{A2}$$

Here, the first term comes from the kinetic energy and the the second term from the Rashba spin-orbit coupling. In the interaction picture, the propagator of the order of $\mathcal{O}(\mathbf{E}^1)$ is

$$U_1^{(\rm I)} = -\frac{i}{\hbar}\int_{-\infty}^{0} dt\ \mathcal{H}_1^{(\rm I)}(t) \tag{A3}$$

where

$$\begin{aligned} \mathcal{H}_1^{(\rm I)}(t) =& e^{i\mathcal{H}_0 t/\hbar}\mathcal{H}_1(t)e^{-i\mathcal{H}_0 t/\hbar} \\ =& -\frac{e(\mathbf{E}\cdot\mathbf{p})}{m}t\exp(\delta t) \\ &+ \frac{\alpha_R}{\hbar}[(e\mathbf{E}\times\boldsymbol{\sigma}^{(\rm I)}(t))\cdot\hat{\mathbf{z}}]t\exp(\delta t), \end{aligned} \tag{A4}$$

and

$$\begin{aligned} \boldsymbol{\sigma}^{(\rm I)}(t) =& e^{i\mathcal{H}_0 t/\hbar}\boldsymbol{\sigma}e^{-i\mathcal{H}_0 t/\hbar} \\ =& \boldsymbol{\sigma}\cos\left(\frac{2\epsilon_k t}{\hbar}\right) + (\hat{\mathbf{n}}\times\boldsymbol{\sigma})\sin\left(\frac{2\epsilon_k t}{\hbar}\right) \\ &+ \hat{\mathbf{n}}(\hat{\mathbf{n}}\cdot\boldsymbol{\sigma})\left[1-\cos\left(\frac{2\epsilon_k t}{\hbar}\right)\right]. \end{aligned} \tag{A5}$$

Here we define

$$\epsilon_{\mathbf{k}} = \left|J\hat{\mathbf{M}} + \alpha_R\mathbf{k}\times\hat{\mathbf{z}}\right|, \tag{A6}$$

and

$$\hat{\mathbf{n}} = \frac{1}{\epsilon_{\mathbf{k}}}\left(J\hat{\mathbf{M}} + \alpha_R\mathbf{k}\times\hat{\mathbf{z}}\right). \tag{A7}$$

Thus,

$$U_1^{(\rm I)}(\mathbf{k}) = U_{1(a)}^{(\rm I)}(\mathbf{k}) + U_{1(b)}^{(\rm I)}(\mathbf{k}), \tag{A8}$$

where

$$U_{1(a)}^{(\rm I)}(\mathbf{k}) = -i\frac{e(\mathbf{E}\cdot\mathbf{k})}{m}\frac{1}{\delta^2}, \tag{A9}$$

and

$$U^{(\mathrm{I})}_{1(b)}(\mathbf{k}) = -\frac{i}{\hbar}\frac{\alpha_R}{\hbar}\left\{\frac{1}{2}[(e\mathbf{E}\times\boldsymbol{\sigma})\cdot\hat{\mathbf{z}}]\left(\frac{1}{(2\epsilon_{\mathbf{k}}/\hbar+i\delta)^2}+\frac{1}{(2\epsilon_{\mathbf{k}}/\hbar-i\delta)^2}\right)\right.$$
$$+\frac{1}{2i}[(e\mathbf{E}\times(\hat{\mathbf{n}}\times\boldsymbol{\sigma}))\cdot\hat{\mathbf{z}}]\left(\frac{1}{(2\epsilon_{\mathbf{k}}/\hbar+i\delta)^2}-\frac{1}{(2\epsilon_{\mathbf{k}}/\hbar-i\delta)^2}\right)$$
$$\left.+[(e\mathbf{E}\times\hat{\mathbf{n}})\cdot\hat{\mathbf{z}}](\hat{\mathbf{n}}\cdot\boldsymbol{\sigma})\left[-\frac{1}{\delta^2}-\frac{1}{2}\left(\frac{1}{(2\epsilon_{\mathbf{k}}/\hbar+i\delta)^2}+\frac{1}{(2\epsilon_{\mathbf{k}}/\hbar-i\delta)^2}\right)\right]\right\}. \quad \text{(A10)}$$

Thus, the change in the state due to the adiabatically turned on electric field is given by

$$\delta\left|\psi_{\mathbf{k},\pm}\right\rangle = U^{(\mathrm{I})}_1(\mathbf{k})\left|\psi_{\mathbf{k},\pm}\right\rangle. \quad \text{(A11)}$$

Now, the spin accumulation arising from the changes in the occupied states is

$$\begin{aligned} s^{\pm}_{\mathbf{k}(2)} &= \frac{\hbar}{2}\left[\left(\delta\left\langle\psi_{\mathbf{k},\pm}\right|\right)\boldsymbol{\sigma}\left|\psi_{\mathbf{k},\pm}\right\rangle + \left\langle\psi_{\mathbf{k},\pm}\right|\boldsymbol{\sigma}\left(\delta\left|\psi_{\mathbf{k},\pm}\right\rangle\right)\right]_{\delta\to 0} \\ &= \frac{\hbar}{2}\times 2\mathrm{Re}\left[\left\langle\psi_{\mathbf{k},\pm}\right|\boldsymbol{\sigma}U^{(1)}_1(\mathbf{k})\left|\psi_{\mathbf{k},\pm}\right\rangle\right]_{\delta\to 0} \\ &= \pm\frac{\hbar}{2}\alpha_R eE\left\{\frac{J}{2\epsilon^3_{\mathbf{k}}}[\hat{\mathbf{M}}\times(\hat{\mathbf{z}}\times\hat{\mathbf{E}})]+\frac{\alpha_R}{2\epsilon^3_{\mathbf{k}}}(\hat{\mathbf{E}}\times\mathbf{k})\right\}, \end{aligned} \quad \text{(A12)}$$

where $\pm$ indicates majority/minority bands, respectively. When the electric field is applied along the $\hat{\mathbf{x}}$ direction, we arrive at Eq. (6). Note that $U^{(\mathrm{I})}_{1(a)}$ does not contribute to the spin expectation value since it is purely imaginary.

* Electronic address: hwl@postech.ac.kr
† Electronic address: kj_lee@korea.ac.kr
(∗∗) These authors equally contributed to this work.

[1] I. M. Miron, K. Garello, G. Gaudin, P.-J. Zermatten, M. V. Costache, S. Auffret, S. Bandiera, B. Rodmacq, A. Schuhl, and P. Gambadella, Nature (London) **476**, 189 (2011).
[2] I. M. Miron, T. Moore, H. Szambolics, L. D. Buda-Prejbeanu, S. Auffret, B. Rodmacq, S. Pizzini, J. Vogel, M. Bonfim, A. Schuhl, and G. Gaudin, Nat. Mater. **10**, 419 (2011).
[3] L. Liu, C.-F. Pai, Y. Li, H. W. Tseng, D. C. Ralph and R. A. Buhrman, Science **4**, 555 (2012).
[4] L. Liu, C.-F. Pai, D. C. Ralph and R. A. Buhrman, Phys. Rev. Lett. **109**, 186602 (2012).
[5] S.-M. Seo, K.-W. Kim, J. Ryu, H.-W. Lee, and K.-J. Lee, Appl. Phys. Lett. **101**, 022405 (2012).
[6] A. Thiaville, S. Rohart, É. Jué, V. Cros, and A. Fert, Europhys. Lett. **100**, 57002 (2012).
[7] P. P. J. Haazen, E. Muré, J. H. Franken, R. Lavrijsen, H. J. M. Swagten, and B. Koopmans, Nat. Mater. **12**, 299 (2013).
[8] S. Emori, U. Bauer, S.-M. Ahn, E. Martinez, and G. S. D. Beach, Nat. Mater. **12**, 611 (2013).
[9] K.-S. Ryu, L. Thomas, S.-H. Yang, and S. S. P. Parkin, Nat. Nanotech. **8**, 527 (2013).
[10] K.-S. Lee, S.-W. Lee, B.-C. Min, and K.-J. Lee, Appl. Phys. Lett. **102**, 112410 (2013).
[11] A. van den Brink, S. Cosemans, S. Cornelissen, M. Manfrini, A. Vaysset, W. van Roy, T. Min, H. J. M. Swagten, and B. Koopmans, Appl. Phys. Lett. **102**, 112410 (2013).
[12] K. Garello, C. O. Avci, I. M. Miron, O. Boulle, S. Auffret, P. Gambadella, and G. Gaudin, arXiv:1310.5586.
[13] K.-S. Lee, S.-W. Lee, B.-C. Min, and K.-J. Lee, Appl. Phys. Lett. **104**, 072413 (2014).
[14] Y. Yoshimura, T. Koyama, D. Chiba, Y. Nakatani, S. Fukami, M. Yamanouchi, H. Ohno, K.-J. Kim, T. Moriyama, and T. Ono, Appl. Phys. Express **7**, 033005 (2014).
[15] J. Linder and M. Alidoust, Phys. Rev. B **88**, 064420 (2013).
[16] M. I. D'yakonov and V. I. Perel, JETP Lett. **13**, 467 (1971).
[17] J. E. Hirsch, Phys. Rev. Lett. **83**, 1834 (1999).
[18] S. F. Zhang, Phys. Rev. Lett. **85**, 393 (2000).
[19] K. Ando, S. Takahashi, K. Harii, K. Sasage, J. Ieda, S. Maekawa, and E. Saitoh, Phys. Rev. Lett. **101**, 036601 (2008).
[20] L. Liu, T. Moriyama, D. C. Ralph and R. A. Buhrman, Phys. Rev. Lett. **106**, 036601 (2011).
[21] Yu. A. Bychkov and E. I. Rashba, JETP. Lett. **39**, 78 (1984).
[22] V. M. Edelstein, Solid State Commun. **73**, 233 (1990).
[23] K. Obata, and G. Tatara, Phys Rev. B **77**, 214429 (2008).
[24] A. Manchon and S. Zhang, Phys. Rev. B **78**, 212405 (2008).
[25] A. Matos-Abiague and R. L. Rodriguez-Suarez, Phys. Rev. B **80**, 094424 (2009).
[26] X. Wang and A. Manchon, Phys. Rev. Lett. **108**, 117201 (2012).
[27] K.-W. Kim, S.-M. Seo, J. Ryu, K.-J. Lee, and H.-W. Lee, Phys. Rev. B **85**, 180404(R) (2012).
[28] D. A. Pesin and A. H. MacDonald, Phys. Rev. B **86**,

014416 (2012).
[29] E. van der Bijl and R. A. Duine, Phys. Rev. B **86**, 094406 (2012).
[30] P. M. Haney, H.-W. Lee, K.-J. Lee, A. Manchon, and M. D. Stiles, Phys. Rev. B **87**, 174411 (2013).
[31] H. Kurebayashi, J. Sinova, D. Fang, A. C. Irvine, T. D. Skinner, J. Wunderlich, V. Novák, R. P. Campion, B. L. Gallagher, E. K. Vehstedt, L. P. Zarobo, K. Vyborny, A. J. Ferguson, and T. Jungwirth, Nat. Nanotech. **9**, 211 (2014).
[32] J. Kim, J. Sinha, M. Hayashi, M. Yamanouchi, S. Fukami, T. Suzuki, S. Mitani, and H. Ohno, Nat. Mater. **12**, 240 (2013).
[33] X. Qiu, K. Narayanapillai, Y. Wu, P. Deorani, X. Yin, A. Rusydi, K.-J. Lee, H.-W. Lee, and H. Yang, arXiv:1311.3032.
[34] X. Fan, H. Celik, J. Wu, C. Ni, K.-J. Lee, V. O. Lorenz, and J. Q. Xiao, Nat. Commun. **5** 3042 (2014).
[35] R. H. Liu, W. L. Lim, and S. Urazhdin, Phys. Rev. B **89**, 220409(R) (2014).
[36] K. Garello, I. M. Miron, C. O. Avci, F. Freimuth, Y. Mokrousov, S. Blügel, S. Auffret, O. Boulle, G. Gaudin, and P. Gambardella, Nat. Nanotech. **8**, 587 (2013).
[37] X. Qiu, P. Deorani, K. Narayanapillai, K.-S. Lee, K.-J. Lee, H.-W. Lee, and H. Yang, Sci. Rep. **4**, 4491 (2014).
[38] J. Sampaio, V. Cros, S. Rohart, A. Thiaville, and A. Fert, Nat. Nanotech. **8**, 839 (2013).
[39] C. O. Pauyac, X. Wang, M. Chshiev, and A. Manchon, Appl. Phys. Lett. **102**, 252403 (2013).
[40] P. M. Haney, H.-W. Lee, K.-J. Lee, A. Manchon, and M. D. Stiles, Phys. Rev. B **88**, 214417 (2013).
[41] J. Sinova, D. Culcer, Q. Niu, N. A. Sinitsyn, T. Jungwirth, and A. H. MacDonald, Phys. Rev. Lett. **92**, 126603 (2004).
[42] J.-i. Inoue, G. E. W. Bauer, and L. W. Molenkamp, Phys. Rev. B **67**, 033104 (2003).
[43] J. Schliemann and D. Loss, Phys. Rev. B **69**, 165315 (2004).
[44] A. A. Burkov, A. S. Núñez and A. H. MacDonald, Phys. Rev. B **70**, 155308 (2004).
[45] E. G. Mishchenko, A. V. Shytov, and B. I. Halperin, Phys. Rev. Lett. **93**, 226602 (2004).
[46] O. V. Dimitrova, Phys. Rev. B **71**, 245327 (2005).
[47] S. Murakami, Phys. Rev. B **69**, 241202(R) (2004).
[48] B. A. Bernevig and S.-C. Zhang, Phys. Rev. Lett. **95**, 016801 (2005).
[49] A. V. Shytov, E. G. Mishchenko, H.-A. Engel, and B. I. Halperin, Phys. Rev. B **73**, 075316 (2006).
[50] A. Khaetskii, Phys. Rev. B **73**, 115323 (2006).
[51] F. D. M. Haldane, Phys. Rev. Lett. **93**, 206602 (2004).
[52] M. Gmitra, A. Matos-Abiague, C. Draxl, and J. Fabian, Phys. Rev. Lett. **111**, 036603 (2013).